A Variational Approach to Exchange Energy Calculations in Micromagnetics

M.J. Donahue
National Institute of Standards and Technology, Gaithersburg, MD 20899, USA

This paper presents a magnetization interpolation method for micromagnetic exchange energy calculations using a variational procedure to relax spins on a supplemental (refined) lattice. The approximations implicit in standard micromagnetic discretization schemes fail when angles between neighboring spins in the model become large, but the proposed approach effectively reduces the angle between neighboring spins, alleviating many of the associated problems. Moreover, this method does not introduce excessive discretization-induced vortex pinning observed with some large angle exchange energy formulations. This paper includes details on proper post-interpolation exchange torque calculation, bounds on nearest neighbor angles for interpolated lattices, a simple model predicting discretization induced Néel wall collapse, and an example of a collapsed (1 cell wide) domain wall that can be restored by the proposed technique.

I. INTRODUCTION

Many difficulties arise in micromagnetic simulations when angles between neighboring spins become large. Nonetheless, computational limitations often prevent many interesting micromagnetic problems from being discretized at a scale fine enough to resolve all the details of the magnetization structure. In particular, models of thin magnetic films often contain vortices and crossties with unresolved cores measuring only a few nanometers across. As discussed below, such undersampled core regions can collapse during model evolution into one cell wide 180° domain walls, even in settings where the Néel wall width is many cells wide. Once formed, these structures are stable, because they tend to be supported by magnetostatic and crystalline anisotropy fields, and the usual exchange energy formulation provides zero torque across 180° spins. One can introduce an exchange energy formulation modified for large angles, but simple approaches result in strong artificial pinning of vortices to the computation grid [1].

One solution to these problems is to base the exchange energy formulation on a continuous interpolation of the magnetization that respects the constraint that the reduced magnetization $\|m\| \equiv 1$. In this paper, an interpolatory "supplemental" lattice is introduced, and a variational procedure is used to relax the spins on this lattice to achieve a smooth interpolation. It is shown that a simple half-step interpolation suffices to avoid the aforementioned one cell wide 180° domain walls, without introducing excessive false pinning of vortices.

II. NÉEL WALL COLLAPSE

Figure 1 shows an example of a situation where an underresolved structure produces errors at a larger scale. This is a simulation of the first μMag standard problem [2], a 20 nm thick, 1 μm $\times$ 2 μm rectangle of $Ni_{80}Fe_{20}$ ($M_s = 8.0 \times 10^5$ A/m, $A = 1.3 \times 10^{-11}$ J/m, $K_u = 500$ J/m^3). The weak uniaxial magneto-crystalline anisotropy is directed along the long axis of the film. The computation cells are 25 nm squares, 20 nm thick, with 3D spins. The exchange energy is given by the 8-neighbor dot product formula $E_i = (A/3)\sum_{n=1}^{8}(1 - m_i \cdot m_n)$, detailed in [1], though similar results are obtained using the more common 4-neighbor expression. The magnetostatic fields are calculated via an FFT-based scalar potential method on an offset grid, described in [3]. The magnetization is relaxed using heavily damped Landau-Lifshitz-Gilbert equations of motion. For more details on the calculation technique, see [4].

The configuration in Fig. 1 is the relaxed state just past the coercive point, after saturation to the left along the long axis of the film. The 180° domain wall in the lower righthand portion of Fig. 1 was formed in an intermediate (non-relaxed) state as part of a vortex + crosstie pair. The vortex drifted upward (behind the inset, but symmetric with the vortex in the opposite corner), and the crosstie flattened out into the observed 1-cell wide domain wall. It is difficult to predict how wide this wall should be, given the restricted spatial dimensions and the complicated magnetic structure, but one certainly expects it to be wider than a single 25 nm cell.

Figure 2 presents a simple illustrative 1D model of a coarsely discretized Néel wall. (See [5,6] for more on 1D wall models, and [7] for a numerical study of 2D wall structures.) In this 4 cell model, each cell is a constant magnetization region, infinite along the y-axis, with width a as shown, and a thickness t small enough to force the spins to lie in the xy-plane. Material parameters are saturation magnetization M_s and exchange constant A. Magneto-crystalline anisotropy is ignored. The outer spins m_1 and m_4 are held fixed and anti-parallel as shown, while the inner spins m_2 and m_3 are allowed to rotate, with θ denoting the angle between the inner spins and their outside neighbor. We make the simplifying assumption that the inner spins are symmetric about the midpoint, as illustrated, because then there are no free poles along the center line, greatly reducing the magnetostatic energy. (This alignment of the center of a Néel wall between discretization nodes is observed in practice.) We also assume that $\theta < 90°$.

Magnetic poles collect along the infinite strip between

the 2 leftmost cells, and between the 2 rightmost cells. This produces a field at spin m_2 that acts against the exchange torque produced on m_2 from m_3. If we include the exchange torque at m_2 from m_1, and solve for 0 torque, we find a unique energy minimum at

$$\sec\theta = 2 - \frac{\mu_0 a^2 M_s^2 \left\{\arctan\left(t/a\right) + \arctan\left[t/(3a)\right]\right\}}{2A\pi},$$

provided the righthand side is > 1. Note that as $a \to 0$, $\theta \to 60^\circ$ as expected. If the righthand side is ≤ 1, then the anti-parallel state ($\theta = 0$) is the only stable configuration, and the Néel wall collapses completely. If M_s, A and t are fixed, then for a sufficiently large the wall will collapse. For a $Ni_{80}Fe_{20}$ film with $t = 20$ nm, this works out to a larger than about 7.1 nm, lending credence to the conjecture that a mechanism of this sort is responsible for the wall collapse observed in Fig. 1.

It seems likely that the under-resolved crosstie formed during the evolution to the relaxed state of Fig. 1 produces a local condition not unlike that modeled in Fig. 2, and seeds the collapse of the entire wall. A similar situation can also arise through grid refinement.

Regardless of its origins, the observed Néel wall collapse is made possible by the disappearance of the exchange torque in the anti-parallel state. One can try a modified exchange field formulation appropriate for large angles, but simple attempts yield unacceptably strong vortex pinning [1]. More sophisticated interpolations of m between grid points are made difficult by the apparent importance of the $\|m\| = 1$ constraint, and the need to produce an interpolation that is consistent across neighboring discretization cells.

A different approach is to interpolate the coarse grid spins $m_1, \ldots, m_N$ with a differentiable function $m(x, y, z)$ that minimizes the variational integral

$$E(m) = A \int (\nabla m_x)^2 + (\nabla m_y)^2 + (\nabla m_z)^2 \, dV, \qquad (1)$$

subject to some constraints. A discrete version of this is developed in the next section. But let us first examine how large an interpolated spin angle can be. As a simple estimate, suppose we are trying to align an interpolating spin $\tilde{m}$ between neighboring spins $m_1, \ldots, m_n$. Consider all of these spins as points in S^2, the unit sphere in $\mathbf{R}^3$. If the angle between $\tilde{m}$ and spin m_i is to be less than θ, then $\tilde{m}$ must lie outside the circular disk symmetrically opposite to m_i on S^2 with diameter $2\pi - 2\theta$. The area of such a disk is $2\pi(1 + \cos\theta)$. This is true for each i, so if the total area of n such disks is less than the total area of the sphere, then there exists a $\tilde{m}$ that is no farther than θ from each of the spins $m_1, \ldots, m_n$. Solving for θ we find $\theta \leq \arccos\left(-1 + 2/n\right)$. As an example, if we are trying to fit $\tilde{m}$ between 4 fixed spins, then there is a direction for $\tilde{m}$ that is at most $\arccos(-1 + 2/4) = 120^\circ$ from each of the fixed spins.

III. THEORY

We now develop a discrete analog to (1). Given the coarse grid spins $\mathbf{m} = (m_1, \ldots, m_N)$, we want to find interpolating spins $\tilde{\mathbf{m}} = (\tilde{m}_1, \ldots, \tilde{m}_{\tilde{N}})$ solving

$$\min_{\tilde{\mathbf{m}}} F(\mathbf{m}; \tilde{\mathbf{m}}) \quad \text{subject to } \Phi(\tilde{\mathbf{m}}) = \mathbf{0}, \qquad (2)$$

where $\Phi = (\phi_k)$ is a collection of constraints, $k = 1, \ldots, K$. (In Section IV we will use $\phi_k(\tilde{\mathbf{m}}) = \|\tilde{m}_k\| - 1$.) We will assume that both the objective function F and the constraints are differentiable.

Let us assume for the moment that the interpolated spins $\tilde{\mathbf{m}}$ are differentiable with respect to $\mathbf{m}$, and use the extended discretization set $(\mathbf{m}, \tilde{\mathbf{m}})$ to evaluate the exchange energy $E(\mathbf{m}) = \tilde{E}\left(\mathbf{m}, \tilde{\mathbf{m}}(\mathbf{m})\right)$.

To relax our solution over $\mathbf{m}$, whether by integrating the Landau-Lifshitz-Gilbert equations, or through direct energy minimization, we need to know $\partial E/\partial \mathbf{m}$:

$$\frac{\partial E}{\partial m_i} = \frac{\partial \tilde{E}}{\partial m_i} + \sum_{j=1}^{\tilde{N}} \frac{\partial \tilde{E}}{\partial \tilde{m}_j} \frac{\partial \tilde{m}_j}{\partial m_i}. \qquad (3)$$

We have only an implicit relation for $\tilde{\mathbf{m}}$ in terms of $\mathbf{m}$, so the last term above is difficult to evaluate. However, suppose we use $\tilde{E}$ as the objective function F in (2). It follows from the theory of Lagrange multipliers that if $(\partial \phi_k/\partial \tilde{m}_j)_{k,j}$ has full rank $K < \tilde{N}$, then at a local minimum $\tilde{\mathbf{m}}$ we can write $\partial \tilde{E}/\partial \tilde{\mathbf{m}}$ as a linear combination of $\partial \phi_k/\partial \tilde{\mathbf{m}}$, i.e.,

$$\frac{\partial E}{\partial m_i} = \frac{\partial \tilde{E}}{\partial m_i} + \sum_{k=1}^{K} \lambda_k \sum_{j=1}^{\tilde{N}} \frac{\partial \phi_k}{\partial \tilde{m}_j} \frac{\partial \tilde{m}_j}{\partial m_i}.$$

If the constraints Φ are independent of $\mathbf{m}$, then the last sum is zero, and we get the simple relation

$$\frac{\partial E(\mathbf{m})}{\partial \mathbf{m}} = \frac{\partial \tilde{E}\left(\mathbf{m}, \tilde{\mathbf{m}}(\mathbf{m})\right)}{\partial \mathbf{m}}.$$

The one difficulty is that we cannot guarantee the differentiability of $\tilde{\mathbf{m}}$ with respect to $\mathbf{m}$. More work needs to be done to identify and handle those spin configurations for which differentiability is lost, but in practice such occurrences appear to be relatively uncommon.

IV. RESULTS AND CONCLUSIONS

To test this interpolation technique, we introduced a supplemental lattice to the simulation described in Section II. The supplemental lattice interpolated the main grid at half the cell dimension, i.e., with 12.5 nm square cells. The 8-neighbor dot product exchange energy formulation was minimized to determine the spins on the supplemental lattice (holding fixed the spins on the original lattice), subject to the constraint $\|m\| = 1$ for all

spins. (For this initial study we employed a simple gradient descent minimization algorithm, which required computation time comparable to that of the demagnetization calculation. We expect a sophisticated minimization algorithm will be much faster.) The refined lattice is used **only** for the exchange energy and exchange torque calculations.

The magnetization configuration in Fig. 1 is not a stable state under the new scheme, but using it as an initial state and allowing the simulation to evolve to a new energy minimum yields Fig. 3. Note that the interpolation has allowed the crosstie to reform, and the domain wall is now a resolved Néel wall. These results are similar to those obtained using the standard exchange scheme and a "real" refinement with 12.5 nm cells. Conversely, using the proposed method the Néel wall doesn't collapse even with 50 nm cells (and a 25 nm supplemental lattice).

As another test, we repeated the vortex pinning simulations detailed in [1], and found no increase in the vortex pinning field.

It is important to distinguish this interpolation technique from a straightforward grid refinement. In the proposed technique the interpolated spins affect only the exchange energy, and at each step the interpolated spins are relaxed completely to an exchange energy minimum (holding fixed the spins on the coarse mesh). Because of this, the angle between neighboring spins on the refined mesh cannot collapse to 180°, as described in Section II. Instead, this technique effectively produces an exchange energy formulation that does not break down in the case of large angles between neighboring spins, yet does not increase vortex pinning.

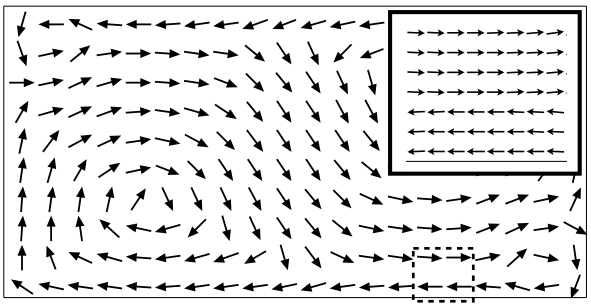

Fig. 1: Simulation results of the μMag first standard problem, using 25 nm square, 20 nm thick calculation cells (4×4 subsample). This is a relaxed state with an applied field of $\mu_0 H = 4.5$ mT directed towards the right. The inset displays all the calculation spins in the dashed box region, showing a collapsed Néel wall.

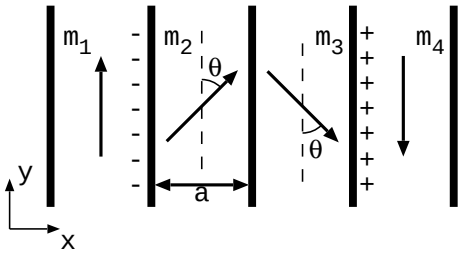

Fig. 2: Illustration of a simple 1D model to study discretization induced Néel wall collapse. The outer spins $\mathbf{m}_1$ and $\mathbf{m}_4$ are fixed and anti-parallel.

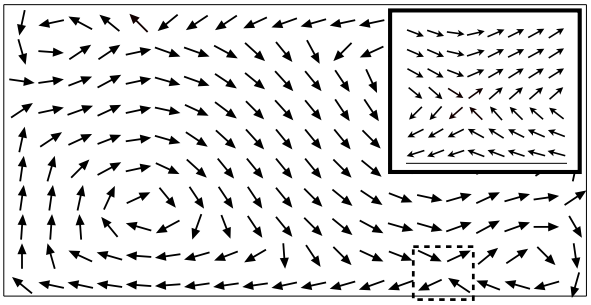

Fig. 3: Simulation results using the described interpolation technique, with Fig. 1 as the initial state ($\mu_0 H = 4.5$ mT). The collapsed wall in that figure has expanded into a crosstie and a resolved Néel wall.

[1] M.J. Donahue and R.D. McMichael, Physica B **233**, 272 (1997).

[2] Round-robin results for a $2 \times 1 \times .02$ μm $Ni_{80}Fe_{20}$ computational problem are available at http://cobalt.nist.gov/mumag/prob1/prob1report.html

[3] D.V. Berkov, K. Ramstöck and A. Hubert, Phys. Stat. Sol. (a) **137**, 207 (1993).

[4] R.D. McMichael and M.J. Donahue, IEEE Trans. Mag. **33**, 4167 (1997).

[5] A. Aharoni, J. Appl. Phys. **37**, 3271 (1966).

[6] W.F. Brown Jr. and S. Shtrikman, Phys. Rev. **125** 825 (1962).

[7] K. Ramstöck, W. Hartung and A. Hubert, Phys. Stat. Sol. (a) **155** 505 (1996).